Mat. Res. Soc. Symp. Proc. Vol. 691 © 2002 Materials Research Society

Pressure Effect of Seebeck Coefficient for Zinc Doped Tin Clathrates

F. Chen[a], K. L. Stokes[a] and G. S. Nolas[b]
[a]Advanced Material Research Institute, University of New Orleans, New Orleans, LA 70108, U.S.A.
[b]Department of Physics, University of South Florida, Tampa, FL 33620, U.S.A.

ABSTRACT

We measured the temperature dependence of electrical resistance (R) and thermopower (S) of $Cs_8Zn_4Sn_{42}$ under high pressure up to 1.2 GPa. Both R and $|S|$ at room temperature increased with pressure. We observed gap widening, irreversible $|S|$ increasing under high pressure, which were similar to the behaviors of Cs_8Sn_{44}. However, the relaxation effect of R for $Cs_8Zn_4Sn_{42}$ was negligible in contrast with that of Cs_8Sn_{44}. We found that the power factor $S^2\sigma$ (σ: electrical conductivity) near room temperature decreased linearly with pressure. The results suggest that the defects in different forms played an important role in transport properties for tin clathrates under high pressure.

INTRODUCTION

There were great efforts to find the thermoelectric materials with better performance in the past decades [1–3]. In the systems that convert heat energy into electric energy (Seebeck effect) or vice versa (Peltier effect), the efficiency is determined by a dimensionless thermoelectric figure of merit $ZT = \frac{S^2\sigma}{\kappa}T$ (κ: thermal conductivity, T: temperature). Compounds of group IV elements that form into clathrate-type structures possess high Seebeck coefficient and electrical conductivity while their thermal conductivity values are low [4], which are good candidates for "electron crystal, phonon glass" (ECPG) [5]. This has stimulated much research interest in these compounds as potential materials for thermoelectric applications [6–8]. Transport properties [9], compressibility, phase transformations [10, 11] and band structure calculations [12] were studied for Si clathrates under high pressure. Thermopower at room temperature for Ge clathrates were reported to increase almost twice under non-hydrostatic pressure up to 7 GPa [13]. Transport properties of Sn clathrates were reported before [4, 14]. Temperature dependence of thermoelectric properties of Cs_8Sn_{44} were measured under hydrostatic pressure up to 1.2 GPa [15]. The band gap of Cs_8Sn_{44} was reported to increase under pressure, and the location of the vacancy sites was proposed to change after application of high pressure [15]. To compare the result, we measured the sample $Cs_8Zn_4Sn_{42}$ and observed a similar irreversible effect on S. The results confirmed a generalized defect picture in $Cs_8A_nSn_{46-n}$, where A = Zn or vacancy.

EXPERIMENTAL DETAILS

The samples were made using powder metallurgy techniques [14, 16]. Briefly, stoichiometric amounts of the the constituent material were reacted at high temperatures (550 °C) in an inert atmosphere. The resulting crystals were ground into a fine powder and the structural properties were measured by x-ray and neutron diffraction. For transport measurements, the powders were hot pressed inside a graphite die at 380 °C and approximately 0.15 GPa for 2.5 hours in an argon atmosphere. This pressure was much lower than the maximum pressure we applied to the samples when doing the transport measurements.

The hydrostatic pressure was generated inside a Teflon cup housed in a Be-Cu high pressure clamp [17]. The 3M Fluorinert was used as the pressure medium in order to get highly *hydrostatic* pressure. The pressure was calculated by the force over area at room temperature. Our previous experiments used superconducting Pb as a manometer to measure pressure near liquid helium temperature and demonstrated that the pressure obtained using this method is within 10% throughout the temperature range 4 K to 300 K [18].

The resistance was measured using dc four-probe method. The resistivity were calculated using the geometrical factors at ambient pressure. The Seebeck coefficient under high pressure was measured using a very low frequency ac two-heater method [19]. Two surface mount resistors were driven by sinusoid currents that differ in phase by $\pi/2$. The amplitude of the currents can be adjusted to minimize the ac component of the base temperature fluctuation ($\tilde{T}$). The ratio ($\delta T/\tilde{T}$) of ac temperature gradient (δT) versus the base temperature fluctuation was monitored to ensure the correct and precise S from ac measurements [19]. Two pairs of T-type thermocouples were attached to the sample directly using pure indium and three independent signals were measured simultaneously to solve for the base temperature, temperature gradient and the Seebeck coefficient. The copper leads of the T-type thermocouples were calibrated relative to Pb using data from Roberts [20]. Our Teflon cell is about 3 mm in diameter and 7 mm long, thus the sample size can be much larger than that could be measured in an anvil cell and ensures precise result together with other careful considerations. Even with the surrounding of fairly good thermally conducting pressure medium, the measured Seebeck coefficient is in good agreement with that was measured outside of the pressure cell. The small pressure effect on thermocouples were also considered and corrected.

RESULTS AND DISCUSSION

Unlike Cs_8Sn_{44}, which showed a very narrow region of positive slope of R–T curve near room temperature, $Cs_8Zn_4Sn_{42}$ showed typical semiconducting behavior throughout our measured temperature range 77 K to 300 K. Figure 1 shows R in logarithm scale versus $1000/T$. The sample was first measured at ambient pressure (curve A in Figure 1). The $\log R$ versus $1/T$ curve was linear from 77 K to 300 K and the energy gap E_g extracted this way was 20.6 meV. After that, the pressure was increased to 0.30 GPa (B), 0.60 GPa (C), 0.90 GPa (D) and 1.20 GPa (E) then decreased to 0.35 GPa (F) and ambient pressure (G). For resistance at 1.20 GPa, only data near room temperature was measured and the R–T curve was not available. Although the temperature range for linear $\log R$–$1/T$ behavior slowly reduced with pressure, the resistance could still be characterized by a well defined energy gap E_g from $T = 150$ K to 300 K. Similar to Cs_8Sn_{44}, both the resistance and E_g increased with pressure. E_g was 20.6 meV, 27.9 meV, 42.6 meV, 56.1 meV, 32.1 meV and 23.2 meV for A, B, C, D, F and G respectively (Table 1). We noticed that E_g at ambient pressure slightly increased after the complete process. We tried to study the relaxation effect of $Cs_8Zn_4Sn_{42}$, which is the resistance relaxation versus time right after change of the

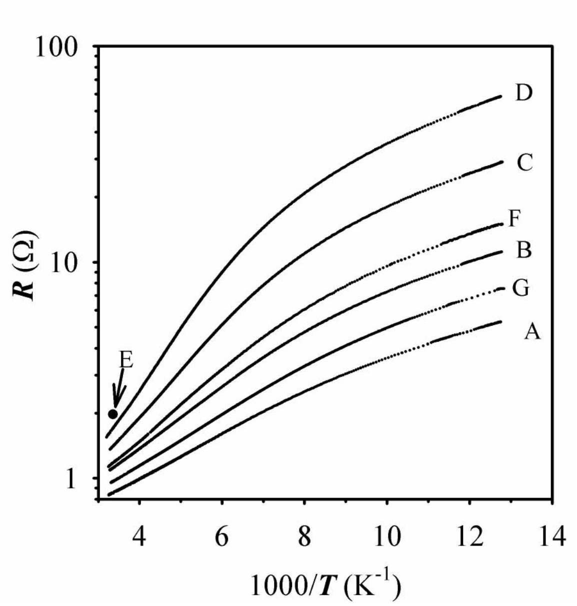

Figure 1: Resistance in logarithm scale versus inverse of temperature for $Cs_8Zn_4Sn_{42}$ under different pressure. The pressure in GPa for each curve/point is A: 0.0, B: 0.30, C: 0.60, D: 0.90, E: 1.20, F: 3.5, G: 0.0 respectively, the sequence of applying pressure is A, B, C, D, E, F and then G.

pressure, that occurred for Cs_8Sn_{44}. The amplitude of the relaxation effect for $Cs_8Zn_4Sn_{42}$ was ∼1%, about 1–2 orders smaller than that of Cs_8Sn_{44}. This can be explained by the factor that Cs_8Sn_{44} has two vacancy sites per unit cell, and the relaxation effect caused by increasing pressure might be directly linked to a vacancy change, while in $Cs_8Zn_4Sn_{42}$ the four defect sites are Zn atoms. The resistance was slightly increased after the pressure sequence A–G. This normally occurs to most polycrystalline samples as micro cracks induced by pressure are typical.

Figure 2 shows S versus T for $Cs_8Zn_4Sn_{42}$ under different pressure. The left graph of Figure 2 shows the curves A, B, C, D and the data point E with pressure increased from 0.0 GPa to 0.30 GPa, 0.60 GPa, 0.90 GPa and 1.20 GPa respectively. $|S|$ increased with increasing pressure. The right graph of Figure 2 shows F (0.35 GPa) and G (0.0 GPa) for better clarity to eyes. The curves A and D were also plotted in the right graph to guide the

Table 1: Comparison of E_g and T' for $Cs_8Zn_4Sn_{42}$ at different pressure. E_g was the energy gap extracted from R–T curve, T' was extracted from S–T curve using Equation 2.

P (GPa)	A: 0.0	B: 0.30	C: 0.60	D: 0.90	F: 0.35	G: 0.0
E_g (meV)	20.6	27.9	42.6	56.1	32.1	23.2
T' (K)	169	131	126	134	133	159
k_BT' (meV)	14.6	11.3	10.8	11.5	11.5	13.7

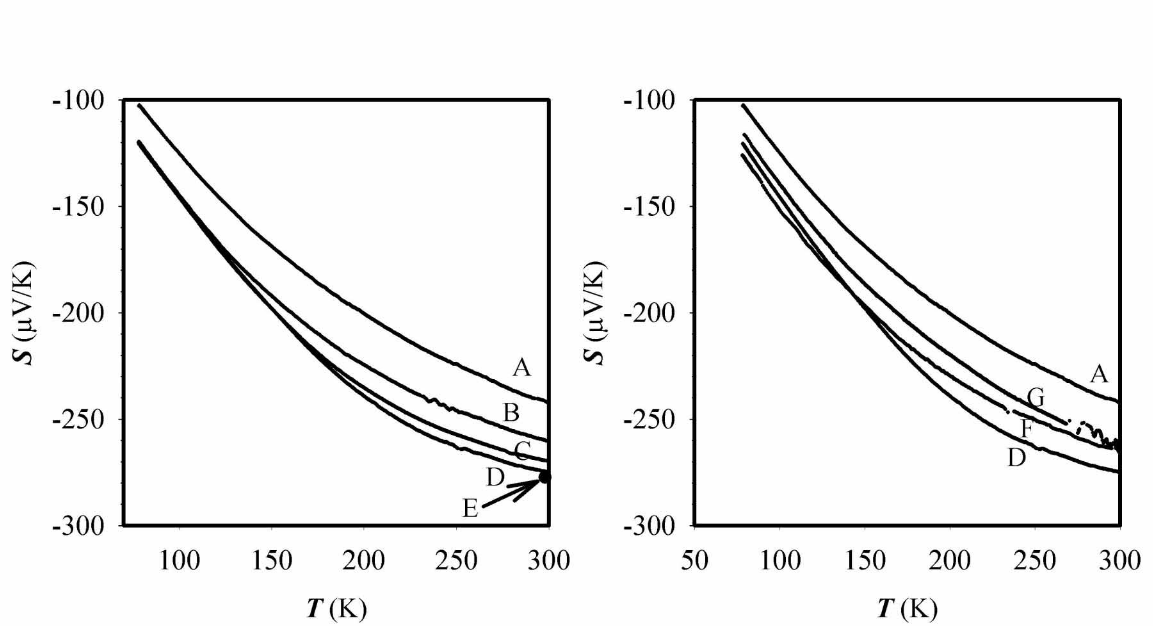

Figure 2: Seebeck coefficient versus temperature for $Cs_8Zn_4Sn_{42}$ under different pressure. The pressure in GPa for each curve/point is A: 0.0, B: 0.30, C: 0.60, D: 0.90, E: 1.20, F: 0.45, G: 0.15 respectively, the sequence of applying pressure is A, B, C, D, E, F and then G. The data were plotted in two graphs of the same scale for clarity.

eyes. Similar to the results for Cs_8Sn_{44}, S was not reversible after the pressure cycle and $|S|$ increased after the pressure was applied and then released. However, the shape of S–T curves for $Cs_8Zn_4Sn_{42}$ are different than Cs_8Sn_{44}. By no means the approximation to a simple degenerate electron gas,

$$S = \frac{k_B}{e}[(r + \frac{5}{2}) - \frac{T^*}{T}), \tag{1}$$

was satisfactory for $Cs_8Zn_4Sn_{42}$. Instead, a purely empirical equation,

$$S = a + b\exp(-\frac{T}{T'}), \tag{2}$$

gave surprisingly good fit to the data under different pressure. Lack of theoretical explanations, this empirical equation may still help understanding the physics of the thermoelectric power due to its nearly perfect fit. We listed the data in Table 1 for comparison with E_g. It turned out that when the pressure increased, E_g increased while k_BT' decreased in general, except increasing from 0.60 GPa to 0.90 GPa. We also noted that Equation 2 was less perfect for $P = 0.90$ GPa.

The power factor $S^2\sigma$ for $Cs_8Zn_4Sn_{42}$ was plotted against temperature for the above mentioned pressures in Figure 3. σ was calculated using the geometrical factors at ambient pressure. $S^2\sigma$ decreased almost linearly near room temperature, thus pressure would not benefit the thermoelectric applications using $Cs_8Zn_4Sn_{42}$ without magic suppression of the lattice thermal conductivity under high pressure, which is unlikely to happen.

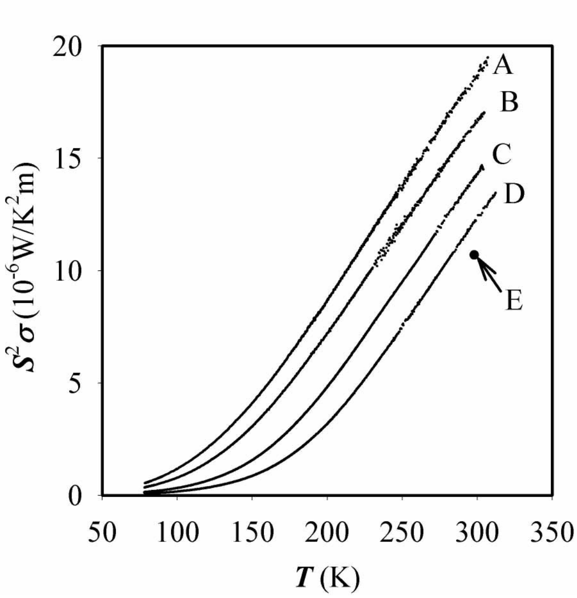

Figure 3: Power factor $S^2\sigma$ versus temperature for $Cs_8Zn_4Sn_{42}$ under different pressure. The pressure in GPa for each curve/point is A: 0.0, B: 0.30, C: 0.60, D: 0.90, E: 1.20 respectively, the sequence of applying pressure is A, B, C, D, E.

Both Cs_8Sn_{44} and $Cs_8Zn_4Sn_{42}$ can be written as $Cs_8A_nSn_{46-n}$. For Cs_8Sn_{44}, A is vacancy and $n = 2$; while for $Cs_8Zn_4Sn_{42}$, A is Zn and $n = 4$. However, the numbers of defects per unit cell are different for these two materials and the nature of the defects is also different. Typically there are three crystallographic sites named for Sn_{46} as 6c, 16i and 24k sites respectively [14, 16]. Nolas *et al* [16] have shown that the two intrinsic vacancies for Cs_8Sn_{44} are at 6c site and Dong *et al* [21] showed from band structure calculations that there might be two favorable configurations for local energy minimum, namely, placing the two vacancies on 6c sites that are on the same hexagonal surface or different hexagonal surfaces. We proposed that, under high pressure, it was possible that the vacancy changes from one 6c site to another site [15]. There were several similar features between Cs_8Sn_{44} and $Cs_8Zn_4Sn_{42}$ under/after high pressure: $|S|$ increasing under high pressure and irreversible after high pressure, reversible gap widening. These can all be well explained by the similarity between their crystallography structures and the general picture of the defects. We also observed different relaxation effects of R, which can be understood by the factor that it is much more difficult to move Zn atoms from one Sn site to another in $Cs_8Zn_4Sn_{42}$ than it is to move vacancies around in Cs_8Sn_{44}.

CONCLUSIONS

We conducted measurements of both electrical resistance (R) and thermoelectric power (S) for $Cs_8Zn_4Sn_{42}$ under hydrostatic pressure up to 1.2 GPa. Both R and $|S|$ at room temperature increased with pressure. We observed gap widening, irreversible $|S|$ increasing under high pressure. These similarities between $Cs_8Zn_4Sn_{42}$ and Cs_8Sn_{44} under/after pressure can be explained by the similarity between their crystallography structures and the similar effect of their defects. The suppression of relaxation effect of R after applying pressure for $Cs_8Zn_4Sn_{42}$ further supports the special role of the vacancies played in Cs_8Sn_{44} under high pressure. The power factor decreased with increasing pressure. Furthermore, we found a simple empirical equation that described the S–T dependence extremely well under different pressure.

ACKNOWLEDGMENTS

This work is supported by research grant DAAD19-99-1-0001 from the Army Research Office.

REFERENCES

[1] D. A. Wright, Nature **181**, 834 (1958).

[2] G. A. Slack and V. G. Tsoukala, J. Appl. Phys. **76**, 1665 (1994).

[3] R. Venkatasubramanian, E. Silvola, T. Colpitts, and B. O'Quinn, Nature **413**, 597 (2001).

[4] J. L. Cohn, G. S. Nolas, V. Fessatidis, T. H. Metcalf, and G. A. Slack, Phys. Rev. Lett. **82**, 779 (1999).

[5] G. A. Slack, *Thermoelectric Handbook*, CRC Press, Boca Raton, FL, 1995.

[6] G. Nolas, *Mater. Res. Soc. Symp. Proc.*, volume 545, MRS, Warrendale, 1999.

[7] J. S. Tse et al., Phys. Rev. Lett. **85**, 114 (2000).

[8] V. L. Kuznetsov, L. A. Kuznetsov, A. E. Kaliazin, and D. M. Rowe, J. of Appl. Phys. **87**, 7871 (2000).

[9] F. P. Bundy and J. S. Kasper, High Temp.-High Press. **2**, 429 (1970).

[10] A. San-Miguel et al., Phys. Rev. Lett. **83**, 5290 (1999).

[11] G. K. Ramachandran et al., Journal of Physics: Condensed Matter **12**, 4013 (2000).

[12] J. Dong, O. F. Sankey, and G. Kern, Phys. Rev. B **60**, 950 (1999).

[13] J. F. Meng, N. V. C. Shekar, J. V. Badding, and G. S. Nolas, J. of Appl. Phys. **89**, 1730 (2001).

[14] G. S. Nolas, J. L. Cohn, and E. Nelson, *Proc. 18th International Conference on Thermoelectrics*, IEEE Press, Baltimore, 1999.

[15] F. Chen, K. L. Stokes, and G. S. Nolas, J. Phys. Chem. Solids (2001), (in press).

[16] G. S. Nolas, B. C. Chakoumakos, B. Mahieu, G. J. Long, and T. J. R. Weakley, Chem. Mater. **12**, 1947 (2000).

[17] C. W. Chu, Phys. Rev. Lett. **33**, 1283 (1974).

[18] F. Chen, Z. J. Huang, R. L. Meng, Y. Y. Sun, and C. W. Chu, Phys. Rev. B **48**, 16047 (1993).

[19] F. Chen, J. C. Cooley, W. L. Hults, and J. L. Smith, Rev. Sci. Instr. **72**, 4201 (2001).

[20] R. B. Roberts, Philos. Mag. **36**, 91 (1977).

[21] J. Dong, O. F. Sankey, and C. W. Myles, (unpublished).